

Photoinduced long-lived charge transfer excited states in AT-DNA strands

L. Martinez-Fernandez, Yuyuan Zhang, Kimberly de La Harpe, Ashley A. Beckstead,
B. Kohler, R.Improta

Supporting information.

1. **Computational Details**

Our calculations have been performed using density function theory (DFT) and its time-dependent version (TDDFT). The M052x^{1, 2} functional has been used throughout our study (unless specified) for geometry optimizations of the ground and excited minima (S_0 and S_1) and subsequent calculations of their absorption energies and frequencies. This functional has been selected due to its capability to provide an accurate description of dispersion interactions, improving the results given by the “standard” functionals also when describing Charge Transfer transitions.³⁻⁶ Furthermore, as detailed below, it has also been successfully applied for the calculation of IR frequencies in similar systems.⁷⁻⁹ We have combined the M052x functional with the 6-31G(d) basis set (unless otherwise specified) for all calculations presented herein (optimizations, absorption energies and frequency calculations). In order to verify the robustness of our conclusions with respect the choice of the density functional, we performed some test calculations using the long-range corrected CAM-B3LYP functional.¹⁰

Solvent effects have been included via implicit models (using Polarizable Continuum Model, PCM)¹¹ and also by combined explicit/implicit models (explicit water molecules + PCM). For the optimization procedure we have exploited the 'standard' LR (linear-response) implementation of PCM/TD DFT, for which analytic gradients are available.¹² Our previous experience in the study of photophysics of nucleic acids,¹³ including the calculations of IR spectra, indicate that the inclusion of some water molecules of the first solvation shell significantly increases the agreement with the experimental results. On the other hand, it is clear that the choice of the number and of the position of the water molecules to be included suffers from some degree of arbitrariness, though experimental results and/or computations adopting explicit solvation methods can provide useful insights on the most suitable computational model. In our case we choose to ‘saturate’ the hydrogen bonding acceptor/donor moieties in the bases, considering 4 water molecules for Thy and 5 for Ade. For what concerns Thy, our choice is consistent with the NMR experiments on Uracil¹⁴ indicating that no water molecule is strongly bonded to C5 and C6 carbon atoms, and that O7 and O8 are coordinated by two and one water molecule, respectively. Furthermore, Car-Parrinello dynamics suggest that the first coordination shell of uracil (up to 2.5 Å) includes 6 water molecules, 4 in the molecular plane (as in Figure 1) and 2

more or less perpendicular to it.¹⁵ The effect of these latter molecules, much less important when Thy is stacked to Ade, should be considered by PCM, which is expected to account for the effect of water molecules that are more distant and/or not directionally bound to the carbonyl oxygen lone pairs.

For what concerns Ade, our choice is consistent with the computational model successfully adopted when studying the IR spectra of the closely related Gua base,¹⁶ and, furthermore, we have checked that the results of excited state calculations on Ade do not qualitatively depend on the exact number of explicit water molecules considered in the computational model.^{17,18}

In any case, we have computed the Difference IR spectra also by using a computational model that does not consider explicit water molecules. As discussed in detail in section 2.4, the results obtained by this model, though less accurate, does not change the main conclusion of our paper, concerning the assignment of the long-living component to a CT state.

When the phosphate groups were considered, we have included Na⁺ atoms as contraions in order to neutralize them.

The quantities relevant for the application of the **Marcus theory** have been computed at the state-specific (SS)PCM/TD-M052X/6-31G(d) level. SS-PCM/TD-DFT calculations provide a much more reliable estimate of dynamical solvation effect than their linear response (LR) counterparts.^{19,20}

1) The intramolecular reorganization energy was computed as the difference between the energy of the ground state (S_0) computed in the S_0 minimum and in AT-CT-min.

2) The solvent reorganization energy was estimated as the difference between the equilibrium (solvent degrees of freedom fully in equilibrium with the excited state electron density) and nonequilibrium (fast solvent degrees of freedom in equilibrium with the excited state electron density, slow solvent degrees of freedom in equilibrium with the ground state electron density) energy for the CT reaction.

3) The energy of the minima for determining the driving force for CR was determined at the solvent equilibrium level. Note that these values are only semi quantitative estimates due to the small computational model adopted for the duplex, the absence of conformational averaging effects, and possible limitations of the adopted computational method (e.g., functional, choice of the basis set)

All the calculations have been performed using Gaussian09 program.²¹

1.1. The IR spectra

Frequency calculations were performed by means of density functional theory (DFT) using the M052X functional. The harmonic frequencies computed by this method are generally overestimated with respect to the experimental

ones: this discrepancy would significantly decrease by extending the basis set and including anharmonic corrections. On the other hand, for computational convenience, we simply scaled by 0.95 the computed frequencies to make easier the comparison with the experimental spectra. As shown in ref.⁷ this level of theory and scaling factor adequately reproduces the ground-state FTIR spectra of DNA duplexes, and has also been successfully applied in other works.⁷⁻⁹ The M052X was combined with the 6-31g(d) basis set but the effect of increasing the basis set to 6-31+G(d,p) was also tested, see section 2.3. Solvent effects are considered into our calculations using an explicit/implicit model: explicitly considering water molecules (see each specific approach for the number of water molecules) and implicitly via a PCM. All labile protons were replaced by deuterons when calculating the IR frequencies. In all cases, for a better comparison between the calculated and experimental IR spectra we have convoluted each computed frequency using a Gaussian function (with Half Width Half Maximum of 5 cm⁻¹).

In previous works, as in ref.⁷, the IR spectra of the charge transfer (CT) states were simulated as the sum of two charged species, however, here we present a more complete study considering different approaches to compute these spectra.

a. The charge transfer state is the “real” S₁ charge transfer minimum in the Adenine-Thymine (ApT) dimer.

In this approach we have modeled the charge transfer state by optimizing the first excited state of this character in the adenine-thymine dinucleotide (S₁ AT-CT-min) surrounded by nine water molecules. In this excited state minimum there is a partial charge transfer between the adenine and thymine bases (see main paper). We have then computed the frequencies for the ground (S₀ AT-min) and first excited (S₁ AT-CT-min) minima at the M052X/6-31G(d) and TD-M052X/6-31g(d) level of theory respectively. In this case we are limited to the small 6-31G(d) basis set since the numerical calculation of the excited state frequencies (analytical frequencies are not yet available) are very demanding. The Difference IR (DIR) spectrum is then obtained by simply subtracting S₀ from S₁ frequencies.

$$DIR = S_1 \text{ AT-CT-min} - S_0 \text{ AT-min}$$

b. The charge transfer state is approached in terms of the cationic and anionic forms of the Adenine-Thymine (AT) dimer.

We are still considering here the AT dimer with nine water molecules but trying to avoid the numerical calculation for the S₁ frequencies, in this case

the charge transfer state is approached as a sum of the AT cation and anion. This methodology has been successfully applied in previous theoretical/experimental studies.⁷⁻⁹ We then performed three optimizations and subsequent frequency calculations (M052X/6-31G(d)) for the ground state of AT: the neutral (S_0 AT-min), the cation (localized in the adenine base, S_0 A⁺pT-min) and the anion (localized in the thymine base, S_0 ApT⁻-min), also including 9 D₂O molecules. The difference spectra is obtained as:

$$DIR = S_0 A^+pT \text{ min} + S_0 ApT^- \text{ min} - [2 \times S_0 AT \text{ min}]$$

It might be considered here that in both the cation and the anion calculations the frequencies corresponding to the “neutral” base are also present. In other words, in the cation although the positive charge is mostly located in the adenine base, we are calculating both the frequencies for this cationic adenine and the neutral thymine. The same occurs in case of the anion calculation. In this respect, the contribution of the thymine frequencies to the cation spectrum has been deleted for simplicity in the Figure 3 of the main paper.

In this case, where the calculations are less demanding, we have also tested the effect of using a larger basis set (6-31+G(d,p)), see section 2.3.

c. The charge transfer state is modeled as sum of the Adenine (dA) cation and Thymine (dT) anion forms of separated nucleotides.

Within this even more simplified approach, we do not consider the AT dimer but the single nucleotides adenine (dA) and thymine (dT) and their charged counterparts (dA⁺ and dT⁻) solvated with 5 and 4 D₂O molecules, respectively. In the same way that in approach b) we here computed both the S_0 neutral and S_0 charged (S_0^+ for dA and S_0^- for dT) for both nucleotides. Then the DIR spectra is calculated as:

$$DIR = S_0 dA^+ \text{ min} + S_0 dT^- \text{ min} - [S_0 dA \text{ min} + S_0 dT \text{ min}]$$

where the ground state (in grey) is computed as the sum of the neutral S_0 for dA and dT. This approach does not account for the effect that the charged base has in the other one, since they are considered in separated calculations. On the other hand, this approach would be the most appropriate to describe a situation where, following the CT formation, the stacking is destroyed, in order to allow a better hydration of the charged moieties.

As in approach b), we have used in this case both M052X/6-31G(d) and M052X/6-31+G(d,p) levels of theory, see section 2.3.

2. Computational Results

2.1. The FC region

As shown in Table S1, the lowest energy excited state in the FC region can be described as a $\pi\pi^*$ transition mainly localized over the Thy base ($T\pi\pi^*$), corresponding to the HOMO \rightarrow LUMO $\pi\pi^*$ intense transition responsible of the lowest energy absorption band of isolated Thy. Analogously S_3 is very similar to the lowest energy $n\pi^*$ transition of isolated Thy. S_2 and S_4 are instead mainly localized over Ade base, corresponding to the so-called L_a and L_b excited states of isolated Ade. Interestingly, the intensity of the L_b excited states is larger than in the isolated Ade, likely due to coupling with the $T\pi\pi^*$ of the close-lying Thy base. S_5 , finally, has a clear $A^+\rightarrow T^-$ CT character (Figure S1). On the other hand, as shown in Figure S1, S_2 transition also exhibits a significant CT character. On the balance this picture is consistent with that obtained by using other computational approaches.²²⁻²⁵

LR-PCM/TD-M052X/6-31G(d) geometry optimizations of S_1 indicates a decay to a minimum very similar to that of $T\pi\pi^*$ in the isolated Thymine. For S_2 geometry optimization predicts instead the decay to AT_{CT-min} .

As anticipated in the main text, several computational and experimental papers²² suggest that AT_{CT-min} is the most likely candidate for being responsible of the long-living component (>50 ps) of the DIR spectrum. Some computational papers^{22, 26, 27} have suggested that monomer-like deactivation channel of Adenine can be slowed down in single strands. On the other hand, in some cases²⁶ the predicted decay time is of the order of ca 5 ps, i.e. slower than of the sub-ps lifetime found for Ade monomer in water but much faster on the 100 ps lifetime measured for the long-living component in $d(AT)_9$. The suggestion that a monomer-like deactivation pathway is responsible of the \sim 100 ps time constant found in oligoAde is not supported by two important experimental findings: (i) the decay constant is very similar in the dinucleotide²⁸ and in $d(AT)_9$, notwithstanding the steric hindrances in the former case should be much smaller (ii) the shape of the long-living and short-living components is different, suggesting the involvement of different type of minima.

Table S1. VAE (in eV), Oscillator strength, and description of the five lowest energy excited state in ApT•9D₂O, according to PCM/TD-M052X/6-31G(d) calculations in water.

	Vertical Absorption Energy(eV)	Osc. Strength	Description
S₁	5.31	0.17	Tππ*
S₂	5.42	0.29	A-I _a
S₃	5.42	0.03	Tnπ*
S₄	5.55	0.17	A-I _b
S₅	5.61	0.01	AT _{CT}

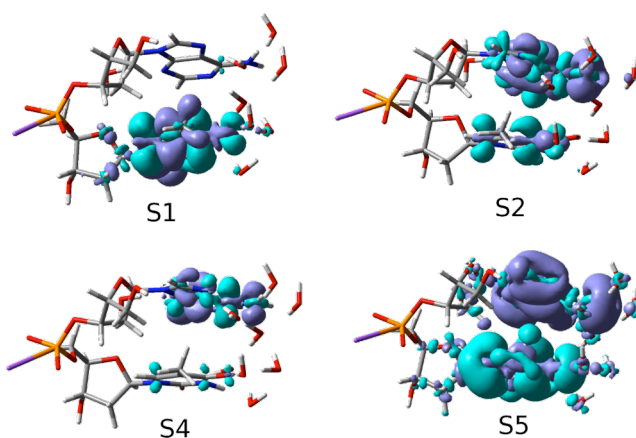


Figure S1: Schematic picture of the electronic density difference (cyan negative, indigo positive) associated to four different electronic transitions in ApT •9 D₂O according to LR-PCM/TD-M052X/6-31G(d) calculations.

2.2. The IR spectra

The (unscaled) frequencies of the IR modes falling in the range monitored by experimental results computed according to approaches a, b and c are summarized in Tables S2-S9.

a. S_1 AT-CT-min and S_0 AT-min.

Table S2. Frequencies (in cm^{-1}) and intensities computed at the S_0 AT-min geometry (without scaling).

S_0 AT-min	Frequency	Intensity
CC,CN (A)	1617	121
CC,CN (A)	1666	171
CC,CN (A)	1705	816
CO (T) ^{asym}	1715	1750
CC (T)	1747	574
CO (T) ^{sym}	1774	691

Table S3. Frequencies (in cm^{-1}) and intensities computed at the S_1 AT-CT-min geometry (without scaling).

S_1 AT-min	Frequency	Intensity
CC,CN (A)	1626	88
CC (T)	1652	242
CO (T) ^{asym}	1684	311
CC,CN (A)		
CO (T) ^{asym}	1694	537
CC,CN (A)		
CO (T) ^{sym}	1702	971

b. S_0 A⁺T⁻-min and S_0 AT⁻-min.

Table S4. Frequencies (in cm^{-1}) and intensities computed at the S_0 ApT⁻-min geometry (without scaling).

S_0 ApT ⁻ -min	Frequency	Intensity
CC,CN (A)	1617	145
CC,CN (A)	1668	207
CO (T) ^{asym}	1679	1033
CO (T) ^{sym}	1703	389
CC (T+A)	1707	1900

Table S5. Frequencies (in cm^{-1}) and intensities computed at the S_0 A⁺pT⁻-min geometry (without scaling).

S_0 A ⁺ pT ⁻ -min	Frequency	Intensity
CC,CN (A)	1620	38
CC,CN (A)	1626	218
CO (T) ^{asym}	1710	1365
CC,CN (A)	1714	258
CC (T)	1748	505
CO (T) ^{sym}	1770	697

c. S_0 dA⁻-min, dA⁺-min, dT⁻-min and dT⁺-min.

Table S6. Frequencies (in cm^{-1}) and intensities computed at the S_0 dA⁻-min geometry (without scaling).

S_0 dA ⁻ -min	Frequency	Intensity
CC,CN (A)	1622	70
CC,CN (A)	1667	207
CC,CN (A)	1706	1354

Table S7. Frequencies (in cm-1) and intensities computed at the **S₀ dA⁺-min** geometry (without scaling).

S₀ dA⁺-min	Frequency	Intensity
CC,CN (A)	1619	62
CC,CN (A)	1626	223
CC,CN (A)	1707	156

Table S8. Frequencies (in cm-1) and intensities computed at the **S₀ dT-min** geometry (without scaling).

S₀ dT-min	Frequency	Intensity
CO (T) ^{asym}	1698	1708
CC (T)	1752	377
CO (T) ^{sym}	1776	853

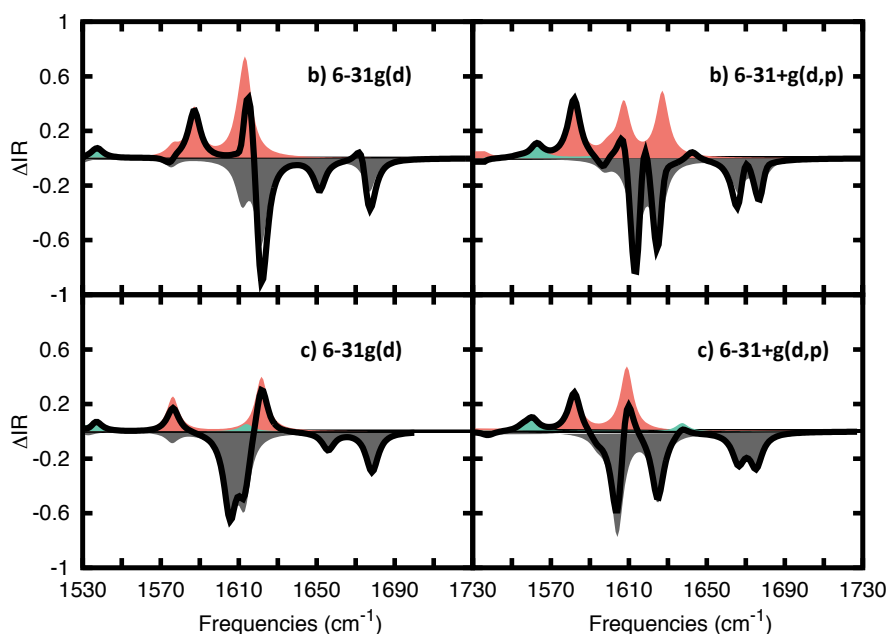
Table S9. Frequencies (in cm-1) and intensities computed at the **S₀ dT⁺-min** geometry (without scaling).

S₀ dT⁺-min	Frequency	Intensity
CO (T) ^{asym}	1557	57
CC (T)	1667	731
CO (T) ^{sym}	1716	1152

2.3. Basis set Effect

When allowed by computational cost of the calculations (approaches b and c), we checked how increasing the basis set from 6-31G(d) to 6-31+G(d,p) changes the computed DIR. Figure S2 depicts the difference IR spectra obtained by using both approaches with the smaller (left) and the larger (right) basis set. In case of the larger basis the scaling factor was set to 0.96. On the balance the increase of the basis set does not dramatically affects the computed DIR. From the quantitative point of view, in the S_0 neutral specie (grey shaded spectra in Fig S2), where 1) the bands at ~ 1650 and ~ 1680 cm^{-1} get closer to each other centered at ~ 1670 cm^{-1} whereas 2) the two bands around ~ 1610 cm^{-1} separate to each other intercalating then a positive feature between them. On the other hand, it is important to highlight that we have used a rather small width (5 cm^{-1}) to simulate the experimental spectrum starting from the computed 'stick' spectrum, especially when considering that we are dealing with high temperature spectra. A slightly larger width would let disappear the very small positive features at 1650 cm^{-1} and 1620 cm^{-1} (b) right panel in Figure S2) leading to a good agreement with the experimental DIR, which exhibits a single and broad positive feature between 1550 cm^{-1} and 1600 cm^{-1} .

Figure S2. Difference IR spectrum (in black solid line) simulated for the AT dinucleotide with $9\text{H}_2\text{O}$ ($\text{ApT}\cdot 9\text{D}_2\text{O}$) following the models b) the S_0 (in shaded gray), the A^+pT (in shade green) and ApT^- (in shaded red) and c) the S_0 (in shaded gray), the $\text{dA}^+\cdot 5\text{D}_2\text{O}$ (in shaded green) and $\text{dT}^-\cdot 4\text{D}_2\text{O}$ (in shaded red). PCM/M052X/6-31G(d) frequencies (scaled by 0.95) left panels and PCM/M052X/6-31+G(d,p) frequencies (scaled by 0.96) right panels.

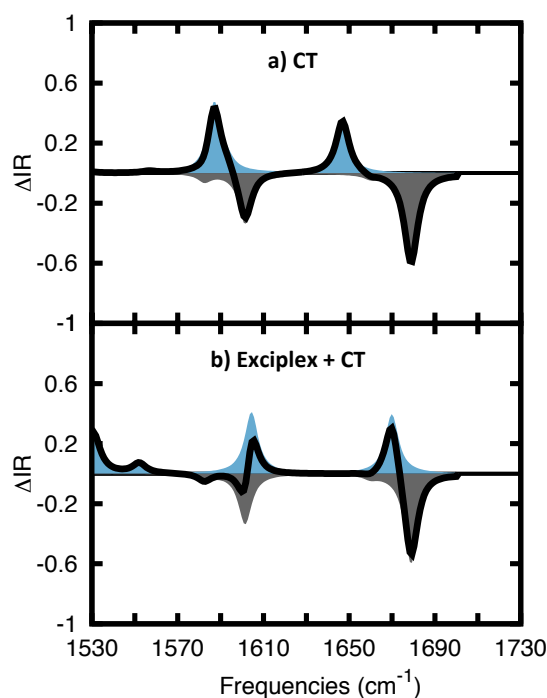


2.4. Explicit solvent Effect

When explicit water molecules are not included into our model, PCM/TD-M052X/6-31G(d) calculations localize two different minima with a substantial CT character, which, however, differs for the degree of CT character. A first minimum is a 'classic' CT (with amount of CT ~ 0.68) similar to that we have described in the main text (AT-CT). The other one (AT-CT_{exc}) is more similar to a 'bonded exciplex', with a smaller CT character (~ 0.40) and a smaller stacking distance between the bases. The DIR spectra relative to both minima are shown in Figure S3.

Comparing the difference spectra of both minima, the DIR computed for AT-CT-min is more similar to the experimental DIR, since it predicts the positive feature at ~ 1600 cm^{-1} . On the other hand, the comparison with the spectrum reported in Figure 2a in the main text show that the shift in the $\text{C}_2=\text{O}$ stretching of Thy due to the presence of an extra negative charge is strongly affected by the explicit inclusion of solvent molecules. It peaks here at 1650 cm^{-1} , i.e. blue-shifted by 30cm^{-1} compared to the calculation including 9 D_2O molecules.

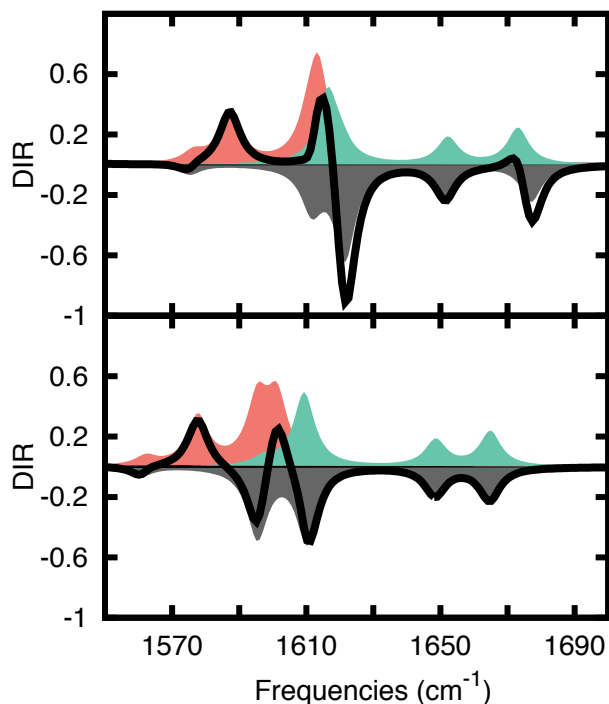
Figure S3. Difference IR spectrum (in black solid line) simulated for the AT dinucleotide following the models a) the S_0 (in shaded gray), the S_1 -min (in shade blue) at the PCM/M052X/6-31G(d) level of theory without explicit water molecules (scaled by 0.95). a) S_1 CT classic charge transfer minimum and b) S_1 minimum with mixed charge transfer and exciplex character.



2.5 Effect of the density functional

The effect of computing the frequencies with the CAM-B3LYP functional, instead of M052X, has been tested by using the approach b) (see Figure S4). The shape of the DIR is very similar, indicating that our conclusions are very robust with respect to the choice of the functional. The only discrepancy between CAM-B3LYP and M052X functionals concerns the frequency of the stretching of the adenine ring (1595cm^{-1}) in the S_0 minimum. Using the CAM-B3LYP functional is shifted in $\sim 20\text{cm}^{-1}$ respect to the M052X spectra, leading to a small extra negative peak in the DIR spectra.

Figure S4. Difference IR spectrum (in black solid line) simulated for the AT dinucleotide with $9\text{H}_2\text{O}$ ($\text{ApT}\cdot 9\text{D}_2\text{O}$) following model b) the S_0 (in shaded gray), the A^+pT (in shade green) and ApT^- (in shaded red) at the PCM/M052X/6-31G(d) level (scaled by 0.95) upper panel and PCM/CAM-B3LYP/6-31G(d) frequencies (scaled by 0.95) lower panel.



3. Experimental Details

The time-resolved infrared (TRIR) spectrometer setup has been described in ref 7. Briefly, the 265 nm pump pulses were produced in an optical parametric amplifier (OPerA solo, Coherent) pumped by 800 nm fundamental (3.5 W, 80 fs, 1 kHz; Libra-HE, Coherent). The signal beam was sum-frequency mixed with 800 nm, producing the prerequisite 530 nm, which was then frequency-doubled to make 265 nm. Every other pump pulse was blocked by a mechanical chopper set at 500 Hz (synchronized to the 1 kHz laser trigger). The pump

beam was attenuated to 3.0 μJ and focused to 500 μm (fwhm) at the sample. The corresponding peak fluence is 1.06 mJ cm^{-2} (assuming Gaussian profile).

The broadband mid-IR probe pulses centered at 6150 nm ($\sim 200 \text{ cm}^{-1}$ bandwidth) were generated by a second optical parametric amplifier (TOPAS + nDFG, Coherent) via difference frequency generation in a GaSe crystal. The probe beam was split into two portion, “signal” and “reference” to minimize shot-to-shot noise. The “signal” beam was attenuated to less than 200 μW and focused to 300 μm (fwhm) at the sample. After the sample, both “signal” and “reference” beams were re-collimated and focused into a spectrograph (Triax, Horiba), dispersed by a 100 grooves/mm grating, and projected onto a liquid N_2 -cooled, dual row 64-element HgCdTe detector.

A translation stage was used to control the optical delay between the pump and probe beams. The relative polarization between the pump and probe was set to magic angle (54.7°). Two milliliter DNA sample solution was recirculated in a temperature-controlled flow cell (Harrick) with an optical pathlength of 100 μm . The front and back CaF_2 windows used in the experiments were 1 mm and 2 mm, respectively. The linear flow rate was set to approximately 0.1 m/s . The temperature of the sample was controlled by an external water bath in which water was flowed through the outside jacket of the temperature-controlled cell. For the duplex experiment, the water bath was set to 5 $^\circ\text{C}$ and the temperature read at the flow cell jacket was 7 $^\circ\text{C}$. For the single strand (melted duplex) experiment, the water bath was set to 85 $^\circ\text{C}$ and the water temperature at the flow cell is 77 $^\circ\text{C}$.

The lyophilized d(AT)₉ sample (gel filtration grade) was purchased from Midland Certified Reagent Company. Approximately 1.05 μmol of single-stranded d(AT)₉ was dissolved in 2 mL of buffered D_2O solution with 100 mM DPO_4^{2-} and D_2PO_4^- phosphate salt and 250 mM NaCl. The resulting concentration was approximately 9 mM per nucleotide (0.25 mM per duplex, 0.5 mM per single strand). Prior to the laser experiments, the solution was heated to 85 $^\circ\text{C}$ for 10 minutes in a water bath and allowed cooled down slowly to room temperature. In addition to the FTIR spectra reported in the main text, the duplex and the single strand were characterized by temperature-ramp UV-visible and circular dichroism (CD) spectroscopy. The UV-visible and CD spectra at various temperatures were shown in Figure S5. The temperature-dependent absorbance at 260 nm (Figure S5c) indicates cooperative melting of the d(AT)₉·d(AT)₉ duplex. The presence of the exciton-coupled CD signal at 70 $^\circ\text{C}$ indicates that although base pairing is disrupted, base stacking is still present above the melting point ($\sim 50 \text{ }^\circ\text{C}$).

Global analysis of the TRIR data was performed using the Glotaran software package.²⁹ The decay-associated difference spectra (DADS) for the d(AT)₉·d(AT)₉ duplex recorded at 7 °C have been described in detail in ref 7. For the d(AT)₉ single strand, a bi-exponential decay was adequate to fit the TRIR data (plus a constant offset to model the solvent heating). The resulting DADS are shown in Figure S6. The uncertainties reported here and in the main text are 2σ (95% confidence interval). The gray trace corresponds to the spectral change arise from the UV pump-induced D₂O heating.

Figure S5. Temperature-ramp CD (a) and UV-visible (b) spectra for d(AT)₉·d(AT)₉ in buffered D₂O solution and 250 mM NaCl. The change in 260 nm absorbance at increasing temperature is shown in panel (c). The spectra were obtained in a 100 μm quartz cell. Data taken from ref 7.

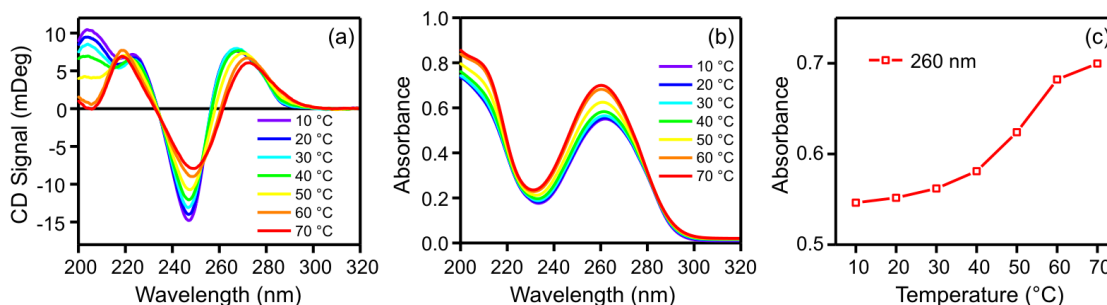
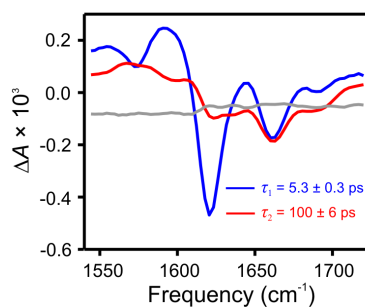


Figure S6. Decay-associated difference spectra (DADS) for single-stranded d(AT)₉ at 77 °C.



References

1. Y. Zhao, N. E. Schultz and D. G. Truhlar, *J. Chem. Theory Comput.*, 2006, **2**, 364.
2. Y. Zhao and D. G. Truhlar, *Acc. Chem. Res.*, 2008, **41**, 157.
3. R. Improta, *Phys. Chem. Chem. Phys.*, 2008, **10**, 2656.
4. R. Improta and V. Barone, *Angew. Chem. Int. Ed. Engl.*, 2011, **50**, 12016.
5. F. Santoro, V. Barone and R. Improta, *ChemPhysChem*, 2008, **9**, 2531.
6. F. Santoro, V. Barone and R. Improta, *J. Am. Chem. Soc.*, 2009, **131**, 15232.
7. Y. Zhang, K. de La Harpe, A. A. Beckstead, R. Improta and B. Kohler, *J. Am. Chem. Soc.*, 2015, **137**, 7059.
8. Y. Zhang, K. de La Harpe, A. A. Beckstead, L. Martínez-Fernández, R. Improta and B. Kohler, *J. Phys. Chem. Lett.*, 2016, **7**, 950.

9. Y. Zhang, J. Dood, A. A. Beckstead, X.-B. Li, K. V. Nguyen, C. J. Burrows, R. Improta and B. Kohler, *Proc. Natl. Acad. Sci. U.S.A.*, 2014, **111**, 11612.
10. T. Yanai, D. P. Tew and N. C. Handy, *Chem. Phys. Lett.*, 2004, **393**, 51.
11. J. Tomasi, B. Mennucci and R. Cammi, *Chem. Rev.*, 2005, **105**, 2999.
12. G. Scalmani, M. J. Frisch, B. Mennucci, J. Tomasi, R. Cammi and V. Barone, *J. Chem. Phys.*, 2006, **124**, 094107.
13. R. Improta and V. Barone, in *Photoinduced Phenomena in Nucleic Acids I*, eds. M. Barbatti, A. C. Borin and S. Ullrich, Springer International Publishing, 2015, vol. 355, ch. 524, pp. 329.
14. M. Chahinian, H. B. Seba and B. Ancian, *Chemical Physics Letters*, 1998, **285**, 337.
15. M.-P. Gageot and M. Sprik, *The Journal of Physical Chemistry B*, 2004, **108**, 7458.
16. Y. Zhang, R. Improta and B. Kohler, *Physical Chemistry Chemical Physics*, 2014, **16**, 1487.
17. T. Gustavsson, N. Sarkar, I. Vaya, M. C. Jimenez, D. Markovitsi and R. Improta, *Photochemical & Photobiological Sciences*, 2013, **12**, 1375.
18. F. Santoro, R. Improta, T. Fahleson, J. Kauczor, P. Norman and S. Coriani, *The Journal of Physical Chemistry Letters*, 2014, **5**, 1806.
19. R. Improta, V. Barone, G. Scalmani and M. J. Frisch, *The Journal of Chemical Physics*, 2006, **125**, 054103.
20. R. Improta, G. Scalmani, M. J. Frisch and V. Barone, *The Journal of Chemical Physics*, 2007, **127**, 074504.
21. M. J. Frisch, G. W. Trucks, H. B. Schlegel, G. E. Scuseria, M. A. Robb, J. R. Cheeseman, G. Scalmani, V. Barone, B. Mennucci, G. A. Petersson, H. Nakatsuji, M. Caricato, X. Li, H. P. Hratchian, A. F. Izmaylov, J. Bloino, G. Zheng, J. L. Sonnenberg, M. Hada, M. Ehara, K. Toyota, R. Fukuda, J. Hasegawa, M. Ishida, T. Nakajima, Y. Honda, O. Kitao, H. Nakai, T. Vreven, J. A. Montgomery Jr., J. E. Peralta, F. o. Ogliaro, M. J. Bearpark, J. Heyd, E. N. Brothers, K. N. Kudin, V. N. Staroverov, R. Kobayashi, J. Normand, K. Raghavachari, A. P. Rendell, J. C. Burant, S. S. Iyengar, J. Tomasi, M. Cossi, N. Rega, N. J. Millam, M. Klene, J. E. Knox, J. B. Cross, V. Bakken, C. Adamo, J. Jaramillo, R. Gomperts, R. E. Stratmann, O. Yazyev, A. J. Austin, R. Cammi, C. Pomelli, J. W. Ochterski, R. L. Martin, K. Morokuma, V. G. Zakrzewski, G. A. Voth, P. Salvador, J. J. Dannenberg, S. Dapprich, A. D. Daniels, A. n. Farkas, J. B. Foresman, J. V. Ortiz, J. Cioslowski and D. J. Fox, *Gaussian 09*, Gaussian, Inc., Wallingford, CT, USA, 2009.
22. R. Improta, F. Santoro and L. Blancafort, *Chem. Rev.*, 2016, **116**, 3540.
23. I. Conti, A. Nenov, S. Hofinger, S. Flavio Altavilla, I. Rivalta, E. Dumont, G. Orlandi and M. Garavelli, *Physical Chemistry Chemical Physics*, 2015, **17**, 7291.
24. F. Plasser, A. J. A. Aquino, W. L. Hase and H. Lischka, *The Journal of Physical Chemistry A*, 2012, **116**, 11151.
25. L. Blancafort and A. A. Voityuk, *The Journal of Chemical Physics*, 2014, **140**, 095102.
26. Y. Lu, Z. Lan and W. Thiel, *Angew. Chem. Int. Ed.*, **50**, 6864
27. I. Conti, P. Altoe, M. Stenta, M. Garavelli and G. Orlandi, *Phys. Chem. Chem. Phys.*, 2010, **12**, 5016.
28. G. W. Doorley, M. Wojdyla, G. W. Watson, M. Towrie, A. W. Parker, J. M. Kelly and S. J. Quinn, *J. Phys. Chem. Lett.*, 2013, **4**, 2739.
29. J. Snellenburg, J., S. Liptonok, R. Seger, K. Mullen, M. and I. Van Stokkum, H.M., *J. Stat. Softw.*, 2012, **49**.

3.1. Optimized minima

Table S10 Coordinates in Angstroms for the different optimized minima.

<hr/> S₁ AT-CT-min + 9H₂O <hr/>			
C	1.14617	-2.69798	0.68104
N	-0.08499	-2.22679	1.05283
C	-0.21955	-0.9789	1.73037
C	0.88389	-0.16434	1.93209
C	2.13401	-0.55998	1.45968
N	2.20784	-1.88275	0.9167
C	-1.2394	-2.94768	0.6125
O	-1.88959	-2.23656	-0.46432
C	-3.17956	-2.839	-0.65049
C	-3.48597	-3.61632	0.64649
C	-2.38526	-3.14528	1.59628
C	-4.18398	-1.76928	-1.0044
O	-4.45518	-0.97816	0.15983
P	-5.3797	0.35121	-0.06068
O	-6.47277	0.08133	-1.05833
O	-3.34902	-4.99796	0.33095
C	0.74643	1.1521	2.65212
O	3.22472	0.1335	1.42084
O	1.30273	-3.80919	0.14023
O	-4.33775	1.40183	-0.76685
C	-3.35541	2.02764	0.06459
C	-2.88396	3.30108	-0.62291
O	-1.87303	2.86589	-1.55124
C	-1.33572	1.63132	-1.15376
C	-2.07402	1.19882	0.11707
N	0.11545	1.83615	-0.93164
C	1.13322	0.93196	-1.1547
C	2.32834	1.65528	-0.85161
N	2.04481	2.90374	-0.47406
C	0.70203	2.98101	-0.54547
N	1.05662	-0.28693	-1.61547
C	2.29325	-0.85267	-1.78797
N	3.46971	-0.30865	-1.61696
C	3.56498	0.96768	-1.13051
N	4.73715	1.51507	-1.01208
C	-2.32664	4.2894	0.39112
O	-1.5584	5.25584	-0.309
O	-5.78652	0.84449	1.30198
Na	-8.07213	0.74311	0.58155
H	-1.32201	5.95562	0.31351
H	-1.71017	3.76961	1.13508
H	-3.1671	4.74942	0.9177
H	-3.66957	3.76552	-1.21534
H	-3.77806	2.21842	1.0511
H	-1.48926	1.45688	0.99865
H	-2.26325	0.12892	0.13536

H	-1.41054	0.90082	-1.95814
H	0.13206	3.88472	-0.36945
H	2.27915	-1.87841	-2.13409
H	4.86613	2.49119	-0.68087
H	5.57535	0.96358	-1.26716
H	-5.10837	-2.23319	-1.34996
H	-3.77684	-1.14038	-1.80038
H	-3.1289	-3.55639	-1.47445
H	-4.4875	-3.3992	1.02052
H	-3.53596	-5.50346	1.13314
H	-2.67715	-2.19782	2.0488
H	-2.15951	-3.87457	2.37363
H	-0.89238	-3.91006	0.24669
H	-1.16608	-0.80984	2.21218
H	3.09914	-2.37214	1.01505
H	1.55586	1.28846	3.36918
H	0.79889	2.00491	1.9688
H	-0.20863	1.20372	3.17708
H	4.77478	-0.64769	1.1105
H	5.60264	-1.43737	0.04219
H	3.70172	1.31277	2.71088
H	3.76111	2.80643	3.00826
H	5.09759	-2.74619	1.53288
H	4.53085	-3.98956	0.79803
H	3.77533	-5.14615	-1.3652
H	2.8635	-4.12121	-0.61772
O	3.7804	-4.27443	-0.9508
O	4.52379	-3.53353	1.65719
O	5.62623	-1.12364	0.9657
O	3.97045	1.94676	3.40591
H	2.83381	3.89152	1.03669
O	3.40548	4.25826	1.7374
H	3.00897	5.10222	1.99016
O	5.34882	4.08906	-0.18535
H	4.79751	4.30076	0.59671
H	5.07865	4.72469	-0.86025
H	4.84399	-1.57533	-1.88821
O	5.53802	-2.22535	-1.66148
H	5.04294	-3.04875	-1.47578
O	7.04368	0.06175	-1.77311
H	6.84258	-0.89116	-1.74868
H	7.22678	0.25488	-2.70155
H	-0.53216	-0.89937	-3.15789
O	-1.43022	-1.24243	-3.06483
H	-1.41487	-1.61676	-2.16662

S₀ AT-CT-min + 9H₂O

C	1.11575	-3.04574	0.63359
N	-0.1384	-2.48527	0.76487
C	-0.3042	-1.22704	1.30149
C	0.71733	-0.45643	1.72972
C	2.05687	-1.00869	1.63005

N	2.14522	-2.28513	1.119
C	-1.29408	-3.21479	0.26714
O	-1.89984	-2.44347	-0.76601
C	-3.26619	-2.87832	-0.91621
C	-3.58083	-3.7444	0.31659
C	-2.42355	-3.43627	1.26412
C	-4.15162	-1.67024	-1.0983
O	-4.18074	-0.92666	0.12678
P	-5.14359	0.39805	0.15649
O	-6.39332	0.17326	-0.64836
O	-3.53891	-5.09521	-0.12536
C	0.55945	0.91718	2.31147
O	3.07857	-0.41212	1.98429
O	1.30676	-4.14979	0.12659
O	-4.24509	1.51118	-0.64551
C	-3.05737	1.9643	0.01175
C	-2.77673	3.41668	-0.36569
O	-1.95274	3.36265	-1.54364
C	-1.27101	2.1418	-1.61433
C	-1.82274	1.23246	-0.50921
N	0.16948	2.37186	-1.4023
C	1.12825	1.40525	-1.53015
C	2.30048	1.96846	-1.04471
N	2.06248	3.25911	-0.61577
C	0.7808	3.45585	-0.84181
N	0.96431	0.1605	-2.00988
C	2.09866	-0.52258	-1.97785
N	3.29822	-0.10827	-1.55973
C	3.46176	1.15266	-1.09127
N	4.66763	1.55453	-0.70959
C	-2.07076	4.14199	0.76787
O	-1.61051	5.38713	0.27073
O	-5.30346	0.79102	1.60064
Na	-7.67205	0.6871	1.32153
H	-1.24933	5.88918	1.01246
H	-1.23612	3.53521	1.14249
H	-2.78312	4.27581	1.58725
H	-3.68535	3.948	-0.64262
H	-3.18158	1.85398	1.09002
H	-1.07843	1.14877	0.27892
H	-2.05186	0.23553	-0.87689
H	-1.38322	1.71604	-2.60926
H	0.2278	4.35683	-0.61813
H	2.0567	-1.54632	-2.33427
H	4.84193	2.53033	-0.46032
H	5.47259	0.95479	-0.89875
H	-5.16089	-1.99376	-1.35448
H	-3.75619	-1.04844	-1.9057
H	-3.34376	-3.50746	-1.80568
H	-4.55315	-3.49762	0.74627
H	-3.72898	-5.6629	0.6336
H	-2.63258	-2.52311	1.8219

H	-2.21808	-4.24989	1.95817
H	-0.91885	-4.15641	-0.12331
H	-1.33179	-0.89244	1.33842
H	3.05578	-2.78391	1.22543
H	1.12151	1.00738	3.2407
H	0.96007	1.67805	1.63348
H	-0.48894	1.13527	2.51388
H	4.88726	-0.90999	1.52923
H	5.62236	-1.56697	0.34042
H	3.34591	1.21926	3.02591
H	3.36455	2.75228	3.001
H	5.07198	-3.00039	1.64708
H	4.5366	-4.20618	0.80975
H	3.99948	-5.31073	-1.46821
H	2.94588	-4.45757	-0.69888
O	3.89141	-4.50517	-0.94743
O	4.42689	-3.74431	1.66075
O	5.71066	-1.37711	1.29949
O	3.45533	1.99177	3.60098
H	2.76901	3.92759	0.95789
O	3.27461	4.19365	1.76043
H	2.84011	4.98828	2.09641
O	5.33057	4.30129	-0.06321
H	4.74274	4.42781	0.70851
H	4.91019	4.81205	-0.76673
H	4.52582	-1.42473	-1.48352
O	5.24275	-2.08741	-1.32808
H	4.8155	-2.96731	-1.32684
O	7.00159	-0.03075	-1.54131
H	6.61595	-0.92398	-1.61454
H	7.09943	0.27258	-2.4524
H	-0.61239	-0.50964	-2.96814
O	-1.44173	-0.97167	-3.18609
H	-1.49476	-1.62433	-2.47171

S₀ A⁺pT-min+ 9H₂O			
C	-0.884772	3.154539	0.651420
N	0.358181	2.567296	0.742949
C	0.524861	1.341219	1.351563
C	-0.489009	0.629128	1.888769
C	-1.817633	1.206608	1.821342
N	-1.904952	2.450277	1.235742
C	1.506156	3.236153	0.146339
O	2.032619	2.384603	-0.870237
C	3.421664	2.718449	-1.083834
C	3.827211	3.641849	0.077495
C	2.686136	3.478918	1.078382
C	4.221016	1.444039	-1.194579
O	4.193282	0.773892	0.073933

P	5.075946	-0.593962	0.221762
O	6.368536	-0.488836	-0.542089
O	3.874655	4.963592	-0.453829
C	-0.323631	-0.696031	2.570449
O	-2.837167	0.657563	2.258352
O	-1.085784	4.234940	0.095850
O	4.145756	-1.701375	-0.553797
C	2.909302	-2.060083	0.068545
C	2.595305	-3.523776	-0.223708
O	1.856003	-3.512202	-1.465438
C	1.222419	-2.286183	-1.649719
C	1.736379	-1.316476	-0.574672
N	-0.245332	-2.479001	-1.48238
C	-1.182615	-1.490401	-1.657743
C	-2.412693	-2.068745	-1.206661
N	-2.217011	-3.321647	-0.79060
C	-0.895912	-3.537599	-0.971366
N	-1.006966	-0.282802	-2.11059
C	-2.164208	0.450452	-2.115727
N	-3.360618	0.071040	-1.747559
C	-3.564427	-1.207490	-1.295987
N	-4.773809	-1.582236	0.988089
C	1.777937	-4.146943	0.894769
O	1.286285	-5.397820	0.432652
O	5.155575	-0.915298	1.691879
Na	7.562758	-1.010505	1.510181
H	0.943906	-5.896899	1.181629
H	0.944932	-3.491691	1.180381
H	2.425208	-4.270715	1.766318
H	3.495590	-4.106298	-0.408334
H	2.979812	-1.877658	1.142580
H	0.953761	-1.136428	0.160852
H	2.042083	-0.357244	-0.985948
H	1.369758	-1.943947	-2.671975
H	-0.379098	-4.455289	-0.71861
H	-2.059136	1.470104	-2.467089
H	-4.997234	-2.535811	-0.64995
H	-5.554353	-0.916495	-1.12363
H	5.251381	1.682291	-1.462812
H	3.791571	0.802117	-1.968953
H	3.513391	3.274240	-2.020135
H	4.793633	3.358907	0.496398
H	4.169645	5.567387	0.236842
H	2.872389	2.607310	1.706800
H	2.548359	4.358612	1.705628
H	1.133815	4.162848	-0.283036
H	1.545008	0.978662	1.355772
H	-2.795057	2.962814	1.334640
H	-0.775287	-0.666574	3.563265
H	-0.823679	-1.490445	2.009565
H	0.730775	-0.946416	2.682322
H	-4.676623	1.134479	1.875036

H	-5.479133	1.690594	0.674348
H	-3.396332	-1.122212	2.826378
H	-3.669253	-2.651061	2.668256
H	-4.884724	3.328921	1.893670
H	-4.370696	4.504781	1.003647
H	-3.826660	5.454678	-1.469610
H	-2.771087	4.644820	-0.654143
O	-3.720664	4.712860	-0.865734
O	-4.206367	4.025682	1.829732
O	-5.516555	1.560816	1.638343
O	-3.879545	-1.871250	3.202808
H	-2.937827	-4.177853	0.891279
O	-3.485169	-4.316944	1.681622
H	-3.131148	-5.083722	2.144140
O	-5.697695	-3.990341	0.052084
H	-5.084160	-4.318518	0.733430
H	-5.893145	-4.731042	-0.53048
H	-4.510797	1.612990	-1.423411
O	-5.154616	2.267232	-1.099429
H	-4.713924	3.135560	-1.121295
O	-6.946340	0.199492	-1.378394
H	-6.640871	1.118856	-1.443673
H	-7.529770	0.040184	-2.126807
H	0.494201	0.729184	-3.147810
O	1.132850	1.407932	-3.402162
H	1.338597	1.858427	-2.569735

S₀ ApT⁻-min+ 9H₂O

C	0.962182	-3.071276	0.56929
N	-0.287951	-2.537168	0.68906
C	-0.519464	-1.341786	1.43211
C	0.572565	-0.605269	1.91983
C	1.851820	-1.121132	1.81571
N	1.972789	-2.386023	1.16412
C	-1.402728	-3.228311	0.10352
O	-1.995131	-2.39236	-0.91058
C	-3.364018	-2.782446	-1.10289
C	-3.717129	-3.729129	0.05691
C	-2.570064	-3.527553	1.03976
C	-4.222725	-1.544102	-1.19148
O	-4.226199	-0.892226	0.08674
P	-5.065589	0.500835	0.21121
O	-6.360259	0.422379	-0.55638
O	-3.725922	-5.05115	-0.48435
C	0.367572	0.736210	2.57298
O	2.956357	-0.603933	2.24623
O	1.186791	-4.140761	-0.04091
O	-4.106213	1.571403	-0.57208
C	-2.874613	1.946518	0.06079
C	-2.592890	3.414799	-0.23765
O	-1.872929	3.411882	-1.48626
C	-1.185546	2.200060	-1.65360

C	-1.684073	1.228234	-0.57270
N	0.260838	2.445137	-1.49277
C	1.229729	1.485240	-1.60531
C	2.411403	2.092721	-1.20215
N	2.172192	3.407693	-0.85035
C	0.877605	3.572471	-1.03709
N	1.074671	0.214361	-2.01205
C	2.219984	-0.451754	-1.97879
N	3.426109	0.002168	-1.61926
C	3.577144	1.286126	-1.22238
N	4.785408	1.724793	-0.87258
C	-1.786245	4.061389	0.87473
O	-1.405746	5.360818	0.43969
O	-5.152049	0.839947	1.67846
Na	-7.549408	0.95435	1.48889
H	-1.029745	5.842043	1.18390
H	-0.900032	3.459995	1.11147
H	-2.414850	4.113608	1.76766
H	-3.509343	3.976975	-0.40965
H	-2.952452	1.764190	1.13405
H	-0.900084	1.067943	0.16633
H	-1.962860	0.254818	-0.97061
H	-1.339186	1.840748	-2.66988
H	0.320788	4.477789	-0.84363
H	2.182210	-1.492967	-2.28349
H	4.921509	2.698720	-0.62329
H	5.593282	1.116790	-0.97952
H	-5.242719	-1.82174	-1.46340
H	-3.821332	-0.86993	-1.95347
H	-3.455158	-3.33549	-2.04222
H	-4.690230	-3.489289	0.48817
H	-3.972761	-5.669032	0.21235
H	-2.774474	-2.668073	1.67782
H	-2.389754	-4.407584	1.65735
H	-1.016694	-4.13705	-0.35141
H	-1.511761	-0.933396	1.33165
H	2.841465	-2.898779	1.28182
H	0.832750	0.772358	3.56042
H	0.814369	1.542101	1.97932
H	-0.697182	0.946125	2.69325
H	4.495374	-1.194869	1.86599
H	5.439631	-1.638792	0.70029
H	3.378300	0.960567	2.95761
H	3.484096	2.518269	2.86219
H	4.914627	-3.366246	1.84821
H	4.436739	-4.484832	0.87482
H	3.787863	-5.157731	-1.62251
H	2.785645	-4.376980	-0.70237
O	3.732298	-4.456235	-0.96645
O	4.397917	-4.194112	1.79835
O	5.380899	-1.594616	1.67024
O	3.771478	1.752386	3.37996

H	2.561801	3.903363	1.06130
O	3.012335	4.128295	1.89383
H	2.429373	4.730043	2.36829
O	4.811183	4.686148	-0.29761
H	4.594591	4.728965	0.64484
H	3.940591	4.643637	-0.72227
H	4.586053	-1.347137	-1.37227
O	5.238572	-2.051599	-1.14141
H	4.767272	-2.902746	-1.17786
O	7.151140	-0.080195	-1.23381
H	6.733966	-0.952921	-1.33070
H	7.709124	0.047767	-2.00637
H	-0.296229	-0.76147	-2.98928
O	-0.933423	-1.40078	-3.35239
H	-1.267471	-1.85526	-2.56372

S₀ dA-min + 5H₂O			
N	0.540782	-2.042713	0.000395
C	0.306134	-0.718694	0.003478
C	1.261775	0.290236	0.008383
C	2.621728	-0.112970	0.010214
N	2.860897	-1.447944	0.003222
C	1.839243	-2.307824	-0.001917
N	0.647615	1.527427	0.003232
C	-0.635506	1.262830	0.000457
N	-0.904637	-0.077894	0.006892
C	-2.230757	-0.677716	-0.024271
C	-3.058024	-0.380805	1.225752
C	-4.474594	-0.389065	0.665458
C	-4.286160	0.211372	-0.728482
O	-2.940173	-0.115144	-1.113692
C	-4.501645	1.707441	-0.807614
O	-3.715896	2.341222	0.194769
O	-4.936455	-1.720412	0.462886
N	3.645258	0.729915	0.016829
H	2.114978	-3.356322	-0.007995
H	3.522366	1.743419	0.035408
H	4.600712	0.366514	0.024258
H	-1.438897	1.985067	-0.015560
H	-2.085938	-1.747160	-0.171726
H	-2.813345	0.608056	1.609721
H	-2.903693	-1.125760	2.006018
H	-4.970865	-2.157014	1.324174
H	-5.176430	0.190018	1.269812
H	-4.968813	-0.277297	-1.425804
H	-4.212705	2.048772	-1.805367
H	-5.565742	1.916303	-0.660356
H	-3.840535	3.295614	0.118024
O	6.405474	-0.220425	0.029507
H	6.201607	-1.182870	0.032168
H	6.714980	-0.040286	-0.866710
O	3.849496	3.607202	0.116945

H	2.951296	4.002967	0.056462
H	4.115515	3.745150	1.034260
H	4.482842	-2.312360	-0.013179
H	-0.779582	-3.467124	-0.044800
O	5.369342	-2.746617	-0.024306
H	5.466984	-3.080567	-0.925062
O	-1.533831	-4.083755	-0.115163
H	-1.669153	-4.173328	-1.066176
H	1.018440	3.340810	-0.011683
O	1.215237	4.305061	-0.011380
H	0.947861	4.609983	0.864868

S₀ dA⁺-min + 5H₂O			
N	0.587701	-2.043528	0.085358
C	0.328834	-0.724606	0.046053
C	1.265721	0.301628	0.030783
C	2.632714	-0.075868	0.059352
N	2.896348	-1.405769	0.095020
C	1.890757	-2.284314	0.104855
N	0.629151	1.526480	-0.018266
C	-0.648795	1.238081	-0.026788
N	-0.893432	-0.106622	0.017178
C	-2.207930	-0.731677	-0.010033
C	-3.054845	-0.412031	1.221095
C	-4.464487	-0.463848	0.645842
C	-4.270955	0.096961	-0.763855
O	-2.914898	-0.216088	-1.124007
C	-4.512826	1.585636	-0.891393
O	-3.750601	2.264281	0.099767
O	-4.899649	-1.809090	0.479445
N	3.640473	0.785804	0.051525
H	2.185691	-3.327206	0.133221
H	3.498655	1.796922	0.039024
H	4.602256	0.440688	0.081140
H	-1.465012	1.944431	-0.073372
H	-2.041888	-1.802253	-0.122835
H	-2.832754	0.592502	1.577067
H	-2.895914	-1.129741	2.025601
H	-4.935319	-2.219879	1.353287
H	-5.183650	0.120443	1.224255
H	-4.936490	-0.425513	-1.453169
H	-4.218478	1.901694	-1.895855
H	-5.582209	1.779052	-0.762494
H	-3.890876	3.213450	-0.008419
O	6.416914	-0.112844	0.125793
H	6.231042	-1.078524	0.153809
H	6.734762	0.047393	-0.771279
O	3.792895	3.667867	0.068257
H	2.888153	4.044594	-0.013368
H	4.045980	3.837524	0.983914
H	4.533484	-2.240111	0.122463

H	-0.705686	-3.492935	0.068049
O	5.427726	-2.658244	0.134257
H	5.542102	-3.016511	-0.755113
O	-1.447664	-4.125365	0.008087
H	-1.571275	-4.244857	-0.941231
H	0.967922	3.344803	-0.082352
O	1.148123	4.311967	-0.108401
H	0.865378	4.637839	0.755392

S₀ dT-min + 4H₂O

C	-2.764669	-0.390664	1.299249
C	-1.951780	-0.840918	0.088690
O	-2.634100	-0.343093	-1.047524
C	-3.989238	0.001365	-0.710470
C	-4.183127	-0.435989	0.744144
N	-0.586851	-0.308811	0.063214
C	-0.404901	1.042944	-0.109215
C	0.812263	1.622228	-0.180358
C	1.969545	0.760131	-0.076042
N	1.712296	-0.581430	0.087048
C	0.475251	-1.177567	0.158972
O	0.342791	-2.388307	0.309508
O	3.139559	1.168486	-0.129557
C	1.021387	3.093168	-0.382052
C	-4.221529	1.475041	-0.962357
O	-3.458516	2.223363	-0.023142
O	-4.671777	-1.772152	0.693584
O	2.289882	-4.162454	-0.943583
O	3.961784	-2.288619	0.381926
O	5.534700	-0.258121	-0.391631
O	4.116560	3.669555	0.887191
H	-5.289883	1.686187	-0.854575
H	-3.919549	1.707263	-1.987042
H	-4.660358	-0.575335	-1.349052
H	-4.872301	0.220402	1.279708
H	-2.503175	0.631405	1.570968
H	-2.621385	-1.044964	2.158782
H	-1.854701	-1.921416	0.037522
H	-1.325437	1.609159	-0.195309
H	0.063662	3.611346	-0.409790
H	1.629596	3.513355	0.419750
H	1.546573	3.281379	-1.321010
H	-4.742296	-2.097351	1.600839
H	2.520542	-1.214805	0.201560
H	3.778204	2.840517	0.509055
H	4.122905	4.279579	0.140362
H	4.752170	0.324746	-0.327408
H	6.122016	0.031151	0.318254
H	4.679785	-1.669516	0.097724
H	4.123101	-2.474297	1.315935
H	1.538259	-3.688770	-0.556330
H	3.046728	-3.667621	-0.591594

H	-3.558832	3.161575	-0.227729
---	-----------	----------	-----------

S₀ dT^{-min} + 4H₂O			
C	-2.814043	0.179184	-1.316990
C	-1.926715	0.775043	-0.225178
O	-2.580385	0.439895	1.007981
C	-3.962779	0.131688	0.779481
C	-4.205725	0.331377	-0.720291
N	-0.579955	0.259760	-0.191188
C	-0.388880	-1.138658	-0.010983
C	0.907347	-1.664869	0.021450
C	1.991420	-0.817679	-0.103878
N	1.711650	0.576090	-0.212084
C	0.469553	1.127790	-0.283567
O	0.319438	2.357741	-0.436095
O	3.255220	-1.142042	-0.119555
C	1.124527	-3.144958	0.196438
C	-4.272216	-1.265067	1.274405
O	-3.607857	-2.210468	0.438531
O	-4.702324	1.663788	-0.879940
O	2.171255	4.066764	0.850461
O	4.164796	2.395597	-0.283318
O	5.034026	0.265163	1.076796
O	4.471620	-3.366495	-0.982947
H	-5.355681	-1.416757	1.242464
H	-3.929432	-1.356953	2.308560
H	-4.578869	0.840986	1.337732
H	-4.922506	-0.391268	-1.114080
H	-2.582748	-0.876498	-1.454585
H	-2.703063	0.705507	-2.265579
H	-1.848594	1.854760	-0.318050
H	-1.282783	-1.701047	0.204182
H	0.193286	-3.631287	0.490920
H	1.470254	-3.614820	-0.728439
H	1.873680	-3.343447	0.966465
H	-4.801613	1.845720	-1.820831
H	2.495264	1.199096	-0.380861
H	3.946541	-2.601766	-0.644922
H	4.148468	-4.142812	-0.517247
H	4.341551	-0.327605	0.631186
H	5.890904	-0.152606	0.951339
H	4.660491	1.697714	0.206739
H	4.694087	2.646820	-1.045673
H	1.460601	3.543630	0.440122
H	2.978922	3.626483	0.543025
H	-3.811872	-3.097451	0.749813
